SANDIA REPORT
SAND2009-5858
Unlimited Release
Printed September 2009

THz Transceiver Characterization: LDRD Project 139363 Final Report

Mark Lee, Michael C. Wanke, Christopher D. Nordquist, Michael J. Cich, Joel R. Wendt, Albert D. Grine, Charles T. Fuller, John L. Reno

Prepared by
Sandia National Laboratories
Albuquerque, New Mexico 87185 and Livermore, California 94550

Sandia is a multiprogram laboratory operated by Sandia Corporation,
a Lockheed Martin Company, for the United States Department of Energy's
National Nuclear Security Administration under Contract DE-AC04-94AL85000.

Sandia National Laboratories

Issued by Sandia National Laboratories, operated for the United States Department of Energy by Sandia Corporation.

Printed in the United States of America. This report has been reproduced directly from the best available copy.

Available to DOE and DOE contractors from

U.S. Department of Energy
Office of Scientific and Technical Information
P.O. Box 62
Oak Ridge, TN 37831

Telephone:	(865) 576-8401
Facsimile:	(865) 576-5728
E-Mail:	reports@adonis.osti.gov
Online ordering:	http://www.osti.gov/bridge

Available to the public from

U.S. Department of Commerce
National Technical Information Service
5285 Port Royal Rd.
Springfield, VA 22161

Telephone:	(800) 553-6847
Facsimile:	(703) 605-6900
E-Mail:	orders@ntis.fedworld.gov
Online order:	http://www.ntis.gov/help/ordermethods.asp?loc=7-4-0#online

SAND 2009-5858
Unlimited Release
Printed September 2009

THz Transceiver Characterization: LDRD Project 139363 Final Report

Mark Lee
Semiconductor Materials and Device Sciences Department

Michael C. Wanke, Joel R. Wendt, Albert D. Grine, Charles T. Fuller
Photonic Microsystems Technology Department

Christopher D. Nordquist, Michael J. Cich
RF/Optoelectronics Department

John L. Reno
Center for Integrated Technologies Science Department

Sandia National Laboratories
P.O. Box 5800
Albuquerque, NM 87185-1415

Abstract

LDRD Project 139363 supported experiments to quantify the performance characteristics of monolithically integrated Schottky diode + quantum cascade laser (QCL) heterodyne mixers at terahertz (THz) frequencies. These integrated mixers are the first all-semiconductor THz devices to successfully incorporate a rectifying diode directly into the optical waveguide of a QCL, obviating the conventional optical coupling between a THz local oscillator and rectifier in a heterodyne mixer system. This integrated mixer was shown to function as a true heterodyne receiver of an externally received THz signal, a breakthrough which may lead to more widespread acceptance of this new THz technology paradigm. In addition, questions about QCL mode shifting in response to temperature, bias, and external feedback, and to what extent internal frequency locking can improve stability have been answered under this project.

Contents

1. Introduction

Only within the last several years has the possibility of an all solid-state infrastructure for photonics at terahertz (THz) frequencies become a realistic concept. This possibility has been due to the invention[1] and continued development[2,3,4,5] of miniature semiconductor quantum cascade lasers (QCLs). Such QCLs are the only coherent solid-state source that can output the many milliwatts of average THz power necessary to transmit through the atmosphere and to supply sufficient local oscillator (LO) power to THz diode receivers[6], with the goal of replacing the gas- and vacuum-tube THz sources most commonly used today. To date all reported THz photonic systems employing QCLs have used discrete source and detector components coupled via mechanically aligned free-space quasioptics[7,8,9], where coupling losses and system size pose significant impediments to practical use. To reach the same maturity level as existing infrared/visible photonics requires integration of solid-state THz sources, detectors, and auxiliary passive and active functionalities onto a compact, chip-based platform amenable to microfabrication methods. Here we report on the first successful monolithic integration of a THz QCL and a solid-state THz mixer to form a simple but generically useful THz photonic integrated circuit (IC) – a microelectronic THz transceiver. This transceiver literally embeds a small Schottky diode into the ridge waveguide cavity of a QCL, so that LO power is supplied to the diode's cathode directly from the QCL's internal fields with no optical coupling path for the LO. We show that this THz photonic IC performs all the basic functions (*e.g.*, transmission of a coherent carrier, heterodyne reception of an external signal, frequency locking and tuning) of discrete component THz photonic systems, but at a small fraction of the size and in a robust platform scalable to semiconductor fabrication production.

2. Transceiver Fabrication and Specifications

The starting point for the integrated transceiver is a THz QCL into which a metal-semiconductor Schottky diode mixer has been directly fabricated, as depicted in Fig. 1. The semiconductor cathode of the Schottky diode and the top bias contact of the QCL ridge waveguide share the same n+ doped GaAs layer. A ≤ 1 μm diameter Ti/Au metal anode is fabricated on the n+ GaAs to define a Schottky contact, while ohmic contact is

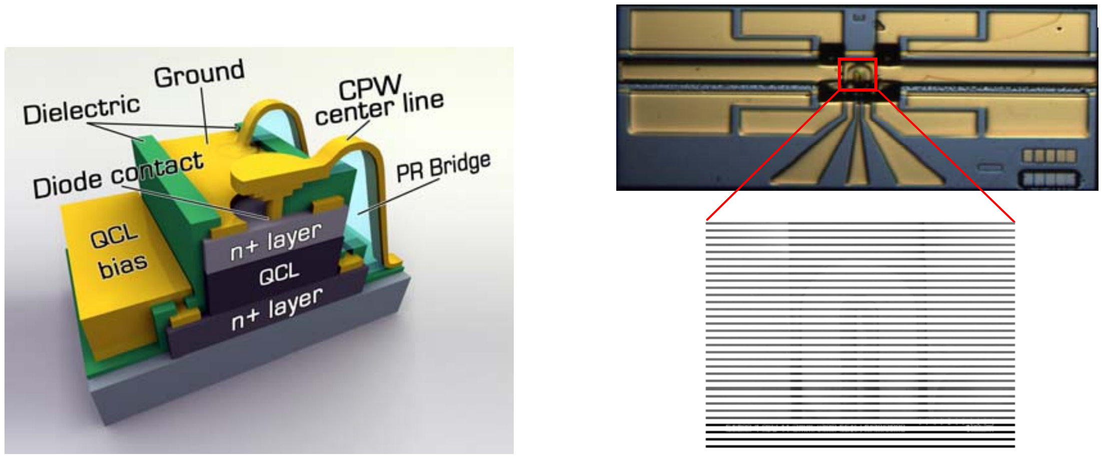

(a) (b)

Figure 1. Design and image of the monolithically integrated THz transceiver. (a) Design drawing showing the Schottky diode position atop a QCL ridge waveguide and ground-signal-ground co-planar waveguide (CPW) intermediate frequency electrode contacts to the diode mixer. (b) (top) Optical microscope plan view image of one complete THz transceiver with all electrical contacts, and (bottom) expanded electron micrograph image showing the CPW contact configuration to the Schottky diode anode.

formed over the remaining area of the *n*+ GaAs layer to form the negative (ground) contact for both laser and diode. This integration strategy has the great advantage that the QCL ridge waveguide cavity's *internal* electric field permeates the diode's cathode and is strongest near the metal-semiconductor interface of the Schottky contact[1]. The internal field is correctly polarized to drive high-frequency currents across the metal-semiconductor contact and hence modulate the width of the diode's depletion region. In addition, if we account for facet reflectances ranging from 30% to greater than 90%[10], the power in the internal THz field is roughly 50% greater than the laser's externally radiated power in a plasmon guided QCL, and over ten times greater in a metal-metal guided QCL. In this way, the QCL supplies LO power to the integrated Schottky diode mixer in the most efficient and physically compact manner possible, eliminating the need for optical alignment between separate source and mixer components. The Schottky diode, if sufficiently small, can be fabricated successfully without significantly degrading the QCL's lasing characteristics. This photonic IC operates as both a coherent THz transmitter and as a heterodyne receiver of external THz signals having frequencies within roughly ± 25 GHz of a QCL mode line. Finally, the integrated diode acts as a very sensitive and high precision probe of the electrodynamics within the QCL resonant cavity. An internally generated signal from this probe can be used, for example, to monitor subtle QCL Fabry-Perot mode frequency shifts in response to changing external conditions, and as feedback to phase lock the modes of a multimode QCL and achieve exceptional differential mode stability.

Fabrication of these integrated transceivers began with molecular beam epitaxy (MBE) growth of a 2.8 THz plasmon waveguided QCL following a design described in Ref. 11, where we used a 4.3 nm wide injection barrier and an average doping of 2.9 x 10^{15} cm^{-3} (sample VB0166). To enable fabrication of a Schottky diode on top of the laser structure, another 40 nm of GaAs doped at 1 x 10^{15} cm^{-3} was grown on top of the 80 nm layer doped at 5 x 10^{15} cm^{-3}. Schottky diodes and associated contacts were integrated as follows. A silicon nitride/oxide stack 320 nm thick was deposited on the QCL material, and e-beam lithography defined 1 µm diameter openings for the Schottky diodes. A reactive ion etch cleared the dielectric stack in the openings down to the GaAs contact, and a Ti/Au (20/100 nm) Schottky anode was sputter deposited to fill the openings. Most of the sputtered metal on top of the dielectric was etched away, leaving only 4 µm diameter circles surrounding the anode contacts. The exposed dielectric stack not under the metal disks was then also etched away. Liftoff was used to produce 165 µm wide ohmic contacts to the top surface of the QCL waveguide, except for a 7 µm diameter opening in the metal around the Schottky diode. Subsequently, another dielectric stack was deposited over the ohmic contact, and separate openings etched through it for access to both the ohmic and Schottky metals. Ridge waveguides 170 µm wide were created using a Cl_2/BCl_3 plasma to etch away the GaAs laser material on both sides of the top metal stripe down to the lower *n*+ contact layer. Liftoff defined the lower contact metal, and the sample was annealed at 380 °C for 30 s to obtain low contact resistance. A second plasma etch was used to remove the lower GaAs *n*+ layer that was not under or between the bottom contact metallization and the laser. This exposed the semi-insulating substrate allowing the use of a high-frequency co-planar waveguide (CPW) to bring the mixer signal off the chip. Another silicon nitride layer was deposited over the structure, with openings etched through it to access the upper and lower ohmic laser contacts and the Schottky diode. A photoresist structure was patterned and reflowed to provide a dielectric bridge from the upper contact and Schottky contact down to the substrate level. Gold was plated to provide a 50 Ω impedance CPW to the Schottky metal, and to bridge from the upper and lower ohmic contacts to wirebond pads. Finally the wafer was thinned to 250 μm to improve thermal conduction and cleaved into 3 mm long bars.

The QCLs were cleaved long enough to ensure multimode operation with Fabry-Perot (F-P) mode spacings close to 13 GHz. This allowed us to diagnose whether the integrated diode coupled properly to the laser by observing the 13 GHz signal from the mixing of periodically spaced internal modes of the laser. The on-wafer 50 Ω CPW was used to access this signal. The center conductor of the CPW was connected to the diode anode and the ground traces were connected to the diode cathode, which was also the QCL ground. The CPW starts on top of the laser ridge, airbridges over the lower contact, and then runs along the substrate to bondpads. The integrated transceiver was wirebonded into a fixture with SMA connectors to maintain a 50 Ω transmission line all the way from the diode to the external microwave measurement equipment. The resulting bandwidth of the microwave test interface was ~ 25 GHz.

Because the diode was driven by fields from the internal modes of the laser, THz energy was not required to flow through any of the metal interconnects above the diode. As a result the upper contact of the diode and the transmission line only required 25 GHz of bandwidth for extraction of the mixing signal, so aggressive reduction of extrinsic capacitance and resistance was unnecessary. Additionally, the extrinsic capacitance between the diode interconnect and the *n*+ laser contact layer defined the THz ground reference for the diode mixer and removed the need for a THz choke on the CPW line.

Post-integration, the DC current-voltage (*I*-*V*) characteristic of each diode was measured to confirm a Schottky contact was formed. The diode *I*-*V*s typically showed ideality factor ≈ 1.9, and total series resistance 140 Ω. The lasing characteristics of the QCLs were also measured after integration processing and still showed robust THz emission after integration of the diodes with no significant change in lasing threshold bias conditions. With the QCLs lasing, diode *I*-*V*s showed a DC offset from rectification of the THz field, indicating the diodes were coupling to the internal fields of the QCLs.

3. Heterodyne Characterization and Signal Reception

Direct proof that the integrated diodes were not only coupling to but also mixing the internal fields of the QCLs is shown in Fig. 2. The QCL for this integrated transceiver

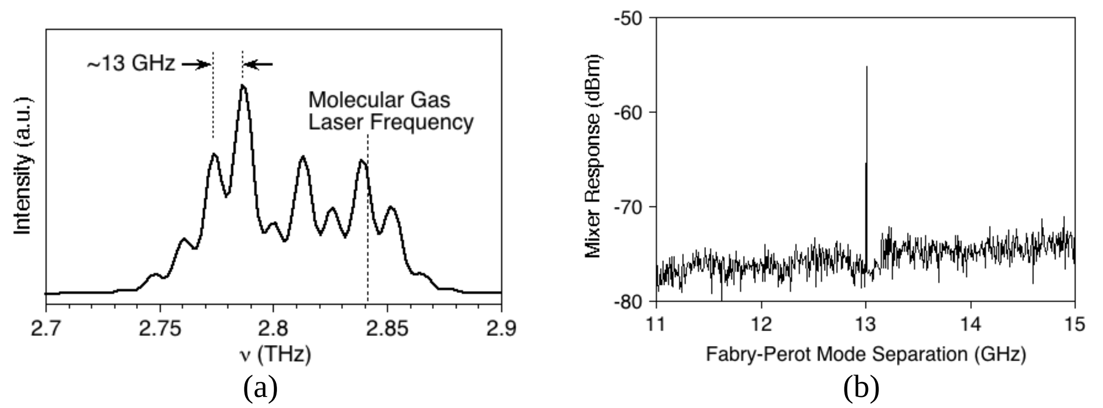

Figure 2. QCL mode difference frequency spectra. (a) Fourier transform spectrum (FTS) of the QCL's multimode emission showing ten Fabry-Perot modes with approximately 13 GHz separation between modes. The frequency of the difluoromethane molecular gas laser line used for the receiver demonstration in Fig 3. is also shown. Spectral resolution of the FTS is 0.25 cm^{-1} (7.5 GHz). (b) Intermediate frequency signal generated by the integrated Schottky diode via the heterodyne downconversion of the internal Fabry-Perot modes of the QCL.

was biased at 0.65 A and 3.0 V to run multimoded, while the diode was operated unbiased. The transceiver IC was cooled in a liquid helium flow cryostat to an operating temperature near 10 K. A Fourier transform spectrum (FTS) (see Fig. 2a) of the QCL transmission shows ten longitudinal mode peaks of varying intensities spaced at approximately 13 GHz intervals around 2.8 THz. 13 GHz is the calculated spacing between F-P modes given the emission frequency, laser cavity index, and QCL length. The intermediate frequency (IF) signal from the diode shown in Fig. 2b was recorded on a microwave spectrum analyzer without an IF amplification chain. With the laser free-running in multimode operation, a clear IF signal peak at 12.961 GHz was observed from the diode's output. This IF signal represents the difference frequency between the laser modes generated by heterodyne downconversion at the diode. It is unclear whether the spectral width of the IF signal in the free running laser is due to small variations in the precise mode spacing between different adjacent modes of the QCL. However, the appearance of this mixing signal shows that the integrated diode clearly responds to 2.8 THz fields.

Operation of the THz IC as a heterodyne receiver is shown in Fig. 3. A separate external signal was supplied by a CO_2-pumped molecular gas laser, using the 2.841143 THz line of difluoromethane. This molecular gas line was used because it lies in the cluster of QCL F-P modes (see Fig. 2a) and therefore is well within ± 25 GHz of at least

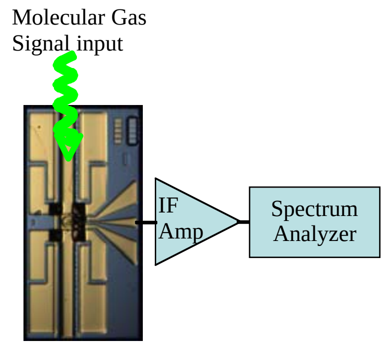

(a)

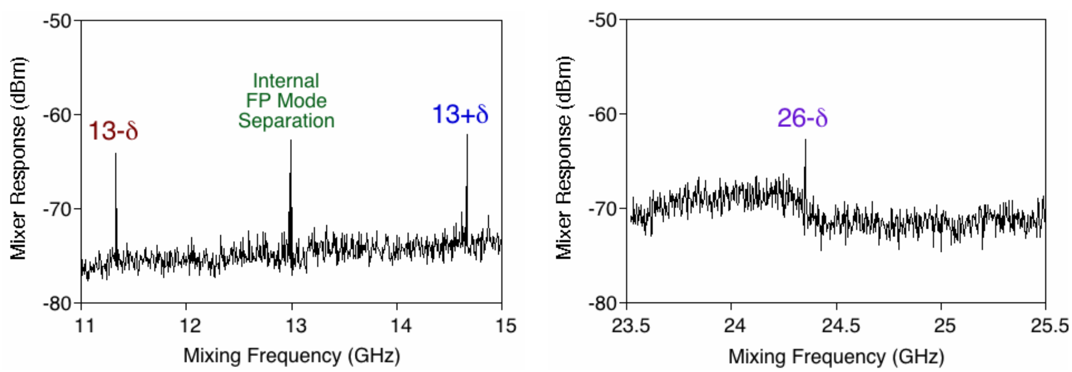

(b)

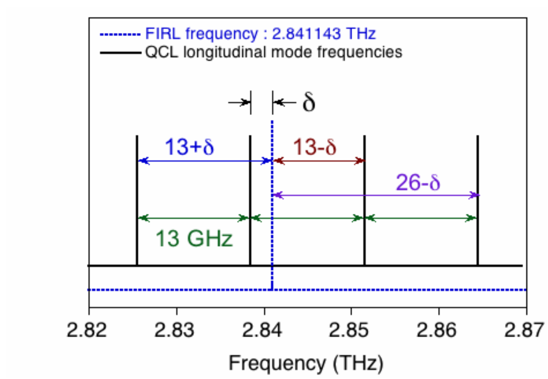

(c)

Figure 3. Heterodyne reception of an external THz signal by the transceiver. (a) Representation of edge facet coupling of the molecular gas laser signal to the transceiver. (b) Intermediate frequency spectra from the integrated diode showing mixing of the internal Fabry-Perot modes at 13 GHz and additional peaks labeled 13-δ, 13+δ, and 26-δ resulting from heterodyne detection of the molecular gas signal. (c) Schematic explanation of the origins of the 13-δ, 13+δ, and 26-δ detected signals as difference frequency mixing products between the difluoromethane line and several of the individual QCL Fabry-Perot modes.

one mode of the QCL, putting the received IF signal within the bandwidth of the IF amplification chain. The external signal is coupled into the integrated transceiver via one edge facet of the QCL ridge waveguide, as sketched in Fig. 3a. Heterodyne reception of the molecular gas laser signal is clearly observed via the peaks labeled as 13-δ, 13+δ, and 26-δ in the IF spectra of Fig. 3b. Note that these signal lines are not sidebands of the QCL's 13 GHz internal difference frequency, but are generated as difference frequencies between the difluoromethane line and three of the QCL's individual F-P mode lines, as explained in Fig. 3c. Here δ is the relatively small (~1.7 GHz) frequency difference between the difluoromethane line and the closest F-P mode of the QCL. The 13-δ and 13+δ signals are then frequency differences between the difluoromethane line and the (respectively) higher and lower adjacent F-P modes, and the 26-δ signal is the difference between the difluoromethane line and the next higher F-P mode.

Sensitivity of this transceiver acting as an integrated heterodyne receiver system was far from optimized as minimum detectable rf power was only about 0.1 μW in a 30 kHz bandwidth. The inefficiency of facet coupling the rf to the device is estimated to reduce sensitivity by three to four orders-of-magnitude, but was necessary as rf coupling structures, such as an antenna, was omitted in this prototype design to simplify fabrication as much as possible. It is also possible that the Schottky diode was underpumped by the QCL LO as the coupling of mixer to QCL fields is strongly dependent on the depth of the Schottky interface into the *n*+ GaAs layer. Such underpumping could significantly degrade the rf-to-IF conversion gain of the diode mixer.

3. Phase Locking to Internal Mode Difference Frequency

Besides enabling heterodyne reception in a monolithic THz IC, the integrated diode can also be used to monitor and control the QCL frequency characteristics, as shown in Fig. 4. Fig. 4a shows the increase in the difference frequency between the diflouromethane laser line and the QCL longitudinal mode at a frequency 13+δ GHz below it with increasing transceiver operating temperature from 10 K to 50 K. Since the frequency of the diflouromethane line is fixed, this frequency increase of the IF signal is generated by a redshift of the QCL's F-P modes with increasing temperature arising from the temperature dependence of the laser cavity index. It is interesting to point out that the entire ~ 1.6 GHz range of this frequency shift is within ¼ of the 0.25 cm^{-1} instrumental linewidth of high-resolution FTS normally used to characterize QCL frequency. Thus the temperature dependence of the QCL frequency is only barely observable using a FTS, but can be mapped out using the integrated diode as a probe at a resolution limited only by the QCL itself (a couple of MHz in this case), rather than by instrumental linewidth.

The F-P mode difference frequency generated by the diode can also be used as an active feedback signal to phase lock the difference modes of the QCL to a microwave

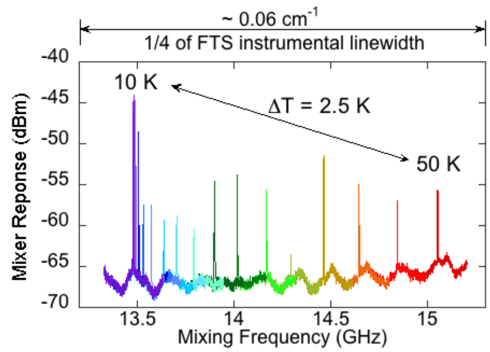

(a)

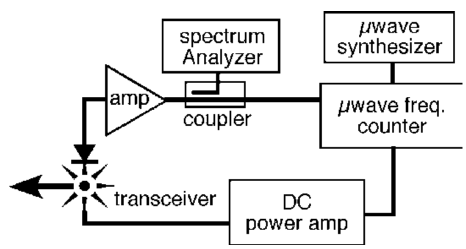

(b)

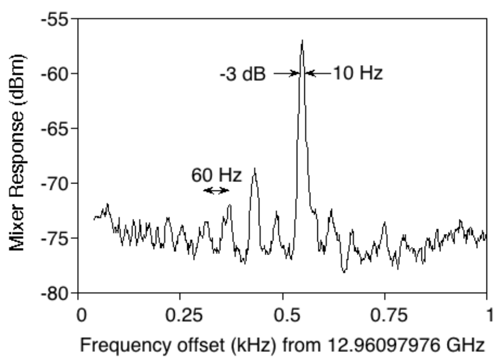

(c)

Figure 4. Monitor and control of QCL using the integrated diode. (a) High precision difference frequency between the diflouromethane laser line and the QCL longitudintal mode at a frequency 13+δ GHz below it at several different operating temperatures between 10 K and 50 K. The Fabry-Perot mode spacing increases approximately 1.6 GHz as temperature is increased over this range. This entire shift is within ¼ of the instrumental linewidth of a FTS. (b) Block diagram of the set-up for phase locking the differential modes of the transceiver using the IF signal from the diode as feedback. (c) High resolution IF spectrum from the integrated diode showing the phase locked differential mode with full-width half-maximum line width of 10 Hz, limited by the instrumental resolution of the spectrum analyzer. The series of smaller peaks are 60 Hz electrical interference.

reference and hence control the transceiver's output frequency. The experimental setup is shown in Fig. 4b. The procedure is similar to that described in Ref. 12, where a superconducting hot electron bolometer mixer was used to generate a F-P difference signal from a QCL using quasioptical coupling between separate source and mixer components in different cryostats. The integrated transceiver significantly simplifies the ability to phase lock by eliminating optical coupling between physically separate components. No mirrors, lenses, windows, or mechanical alignment are required, and the transceiver sits in a single cryostat. Fig. 4c shows the IF spectrum of a phase locked integrated transceiver. The linewidth of this IF signal is ≤ 10 Hz (at full width half-maximum), limited by the instrumental resolution bandwidth of the spectrum analyzer.
The IF frequency of the locked system was also observed to drift < 10 Hz over a period of 10 minutes. Thus the integrated diode can be used to control the differential mode frequency characteristics of the QCL with a very high degree of precision.

4. References

[1]Köhler, R., Tredicucci, A., Beltram, F., Beere, H. E., Linfield, E. H., Davies, A. G., Ritchie, D. A., Iotti, R. C., & Rossi, F. *Nature*, **417**, 156–159, (2002).

[2]Williams, B. S. *Nat. Phot.* **1**, 517-525 (2007)

[3]Kumar, S., Hu, Q., & Reno, J. L. *Appl. Phys. Lett.* **94**, 131105 (2009).

[4]Williams, B. S., Kumar, S., Hu, Q., & Reno, J. L. High-power terahertz quantum-cascade lasers. *Elec. Lett.* **42**, 89-91 (2006).

[5]Walther, C., Fischer, M., Scalari, G., Terazzi, R., Hoyler, N., & Faist, J. *Appl. Phys. Lett.* **91**, 131122 (2007).

[6]Siegel, P. H., Smith, R. P., Gaidis, M. C., & Martin, S. C. *IEEE Trans. Microw. Th. & Tech.* **47**, 596–604 (1999).

[7]Hübers, H.-W., Pavlov, S. G., Semenov, A. D., Köhler, R., Mahler, L., Tredicucci, A., Beere, H. E., Ritchie, D. A., & Linfield, E. H. *Optics Express* **13**, 5890–5896 (2005).

[8]Gao, J. R., Hovenier, J. N., Yang, Z. Q., Baselmans, J. A., Baryshev, A., Hajenius, M., Klapwijk, T. M., Adam, A. J. L., Klaassen, T. O., Williams, B. S., Kumar, S., Hu, Q., & Reno, J. L. *Appl. Phys. Lett.* **86**, 244104 (2005).

[9]Lee, M., Wanke, M. C., Lerttamrab, M., Young, E. W., Grine, A. D., Reno, J. L., Siegel, P. H., & Dengler, R. J. *IEEE J. Sel. Top. Quant. Elec.* **14**, 370–373 (2008).

[10]Kohen, S., Williams, B. S., & Hu, Q. *J. Appl. Phys.* **97**, 053106 (2005).

[11]Alton J., Barbieri, S., Worrall, C., Houghton, M., Beere, H. E., Linfield E. L., & Ritchie, D. A. *Proc. of SPIE* **5727**, 65-73 (2005)

[12]Baryshev, A., Hovenier, J. N., Adam, A. J. L., Kasalynas, I., Gao, J. R., Klaassen, T. O., Williams, B. S., Kumar, S., Hu, Q., & Reno, J. L. *Appl. Phys. Lett.* **89**, 031115 (2006)

Distribution

1	MS 0123	LDRD Office, 01030
1	MS 1415	Mark Lee, 01123
1	MS 1082	Michael C. Wanke, 01725
1	MS 1082	Albert D. Grine, 01725
1	MS 1082	Joel R. Wendt, 01725
1	MS 1082	Charles T. Fuller, 01725
1	MS 1085	Christopher D. Nordquist, 01742
1	MS 1085	Michael J. Cich, 01742
1	MS 1303	John L. Reno, 01132
1	MS 1086	Dan L. Barton, 01123
1	MS 1086	01123 Department File
1	MS 1085	Charles T. Sullivan, 01742
1	MS 1315	Sean J. Hearne, 01132
1	MS 1421	Jerry A. Simmons, 01120
1	MS 1071	C. Andy Boye, 01720
1	MS 1315	Robert Q. Hwang, 01130
1	MS 1427	Julia M. Phillips, 01100
1	MS 1079	Gilbert V. Herrera, 01700
1	MS 0161	Patent and Licensing Office, 1150
1	MS 0899	Technical Library, 9536 (electronic copy)